

# Dynamics of a nanoparticle as a one-spin system and beyond

H. Kachkachi

*Laboratoire de Magnétisme et d'Optique, Université de Versailles St. Quentin,  
45 av. des Etats-Unis, 78035 Versailles, France*

---

## Abstract

We review some recent results beyond the now established theory of magnetization switching of a nanoparticle within the single-spin approximation. The first extension is that of the Stoner-Wohlfarth model for magnetization static switching under applied magnetic field including the effect of temperature at long-time scales. The second concerns a generalization of the Néel-Brown model for thermoactivated dynamic magnetization switching to include the effect of exchange interaction in the framework of Langer's theory in the intermediate-to-high damping limit. We finally argue why the single-spin approximation is not appropriate for very small nanoparticles.

*Key words:* nanomagnetism, magnetization dynamics, exchange interaction  
*PACS:* : 75.50.Tt - 75.10.Hk - 05.40.Jc

---

## 1 Introduction

Magnetic nanoparticles are very interesting and challenging systems to both fundamental research in physics and technological applications. From the point of view of fundamental physics, nanoparticles are interesting because they offer a rich laboratory for the study of dynamic phenomena as they show superparamagnetism at high temperature and exponentially slow relaxation at low temperature. On the other hand, due to their high coercivity, their magnetization enjoys long-range stability, a very important property for the information-storage technology. In principle, particles of very small size may be used to increase the storage density. However, this is hampered by many difficulties related with the finite size of the particles. In particular, surface and thermal

---

*Email address:* kachkach@physique.uvsq.fr (H. Kachkachi).

effects become dominant in such particles, and drastically affect the magnetization relaxation time, and thereby the stability of the information stored in recording media. Therefore, the aim of any study of such systems, be it experimental or theoretical, is to understand the dynamic properties of small nanoparticles taking account of spatial inhomogeneities due to, e.g., surface disorder. For this purpose one has to tackle the difficult problem of including surface effects in the calculation of the relaxation time of the particle magnetization. However, this requires a microscopic approach to account for the local environment inside the particle, and thus include microscopic interactions such as spin-spin exchange, together with magnetocrystalline anisotropy and Zeeman interaction. Unfortunately, this leads to a rather difficult task owing to the large number of degrees of freedom which hinders any attempt to analyze the energyscape. For this reason, *inter alia*, calculations of the reversal time of the magnetization of fine single-domain ferromagnetic particles initiated by Néel [1], and set firmly in the context of the theory of stochastic processes by Brown [2], [3], have invariably proceeded by ignoring all kind of interactions. Thus, the only terms which are taken into account in these calculations are the internal magneto-crystalline anisotropy of the particle, the random field due to thermal fluctuations, and the Zeeman term. This assumes that the particle's atomic moments (or spins) switch in a coherent manner, so that the magnetic state of the particle can be described by a giant magnetic moment, this is the *one-spin approximation*, and the particle is then dealt with as a one-spin system.

It is well known that the magnetization of a nanoparticle can overcome the energy barrier, due to magneto-crystalline anisotropy, and thus reverse its direction, at least in two ways <sup>1</sup>: either under applied magnetic field which suppresses the barrier, or by thermal effects which produce statistical fluctuations. Within the framework of the one-spin approximation, the magnetization switching under applied magnetic field, at zero temperature, is well described by the Stoner-Wohlfarth model [5]. This model has been confirmed by experiments on single cobalt particles by Wernsdorfer et al. [see Ref. [6] for a review]. At finite temperature, but at long-time scales or quasi-equilibrium, this switching occurs according to two regimes. At very low temperature, this is due to the coherent rotation of all spins, as in the Stoner-Wohlfarth model, whereas at higher temperature, the magnetization switches by changing its magnitude <sup>2</sup>. This results in a shrinking of the Stoner-Wohlfarth astroid as predicted by the modified Landau theory [7], and confirmed by experiments [6]. At short-time scales, and within the one-spin approximation, crossing of

---

<sup>1</sup> It has quite recently been shown [4], experimentally and theoretically, that efficient magnetization switching can be triggered by transverse field pulses of a duration that is half the precession period.

<sup>2</sup> Rigorously, the switching of magnetization through a change of its magnitude cannot, however, be explained within the single-spin approximation [see section 4].

the energy barrier activated by thermal energy is described by the Néel-Brown model [1], [2], [3] and its extensions [see section 2.3], again in agreement with experiments on individual cobalt particles [6].

In both Stoner-Wohlfarth and Néel-Brown models, the energy of a fine single-domain ferromagnetic nanoparticle only contains the internal magneto-crystalline anisotropy and the Zeeman term. The thermoactivated dynamics of the particle, e.g., within the stochastic Langevin approach, are described by adding a stochastic field in the equations of motion of the magnetization, in order to account for thermal effects exerted on the particle by the surrounding bath. This stochastic field is responsible for the statistical fluctuations of the magnetization direction.

In this paper we briefly describe these two models. Then, we present two extensions thereof: the first is of the Stoner-Wohlfarth model to include thermal effects on the magnetization switching at long-time scales, or equivalently, at quasi-equilibrium. The second extension is that of the Néel-Brown model which takes account of exchange interaction and investigates its effect on the relaxation time of a pair of magnetic moments, within Langer's approach. It will be shown that the Néel-Brown result for the relaxation time of a rigid magnetic moment is only recovered for very large exchange coupling, while for weak coupling there appear new interesting features, giving a foretaste of the intricacies and subtleties that should arise in a particle when treated as a multi-spin system.

The paper is organized as follows: In section 2 we deal with a nanoparticle in the single-spin approximation. For such a single-spin system, we briefly discuss the Stoner-Wohlfarth model describing the magnetization switching under the applied magnetic field and then consider the effect of temperature within the framework of Landau's theory. Next, the Néel-Brown model for thermoactivated switching is reviewed. We comment on the applicability of this model, and its further extensions to non-axially symmetric potentials, to the calculation of the blocking temperature of an assembly of nanoparticles. In section 3, we abandon the single-spin approximation and deal with the simplest, though non trivial, problem of two exchange-coupled spins and study the effect of the latter on the relaxation time within Langer's approach. The results are then compared with those of the Néel-Brown model. The last section motivates and discusses the generalization of the latter work to a multi-spin particle.

## **2 Magnetization switching of a nanoparticle as a single-spin system**

Before we proceed, we would like to stress the role of anisotropy. Exchange energy is completely isotropic, that is it does not depend on the direction in

space in which the crystal is magnetized. One often chooses the reference  $z$  direction as the one along which the component of the magnetization is calculated. However, this direction does not really have any meaning in the limit of zero applied field. In fact, due to global rotation the net magnetization vanishes in zero applied field. This not only contradicts experiments but it is also in conflict with everyday experience that, for instance, the particles in an audio or video tape remain magnetized, and do not lose the recorded information upon switching off the writing field. This is so because real magnetic materials are not isotropic, and that the reference  $z$  direction in question is actually defined by anisotropy. There are several types of anisotropy, but the most common is the magneto-crystalline anisotropy, caused by the spin-orbit interaction. Indeed, the electron orbits are linked to the crystallographic structure, and by their interaction with the spins they make the latter prefer to align along well-defined crystallographic axes. There are therefore some directions in space in which it is energetically more favorable to magnetize a given crystal than in other directions, the difference being given by the direction-dependent anisotropy energy. As for the exchange interaction, quantitative estimates of the spin-orbit interaction from basic principles are also possible but the accuracy is not as good. Therefore, the anisotropy term is always written as a phenomenological expression, which is actually the first term of a power series expansion that take into account the crystal symmetry, and the corresponding coefficient is usually taken from experiment. The magneto-crystalline energy is usually 2 – 4 orders of magnitude smaller than exchange energy, but the direction of the magnetization is determined only by anisotropy. On the other hand, exchange coupling tends to align all the spins inside the particle parallel to each other, while anisotropy tends to align them along a certain crystallographic direction. A compromise between exchange and anisotropy is obtained by aligning all spins parallel to each other and to the anisotropy direction.

Other features of a magnetic material, namely its subdivision into domains, is then caused but yet another energy term, called the magnetostatic self-energy (demagnetization or shape energy). This is the surface term that stems from the dipolar interactions. It is irrelevant for spherical samples. However, for many materials, slight deviation from spherical shape renders the shape anisotropy very important especially for the spatial dependence of the magnetization. On the other hand, as shown by Brown and Morrish in [8], a single-domain particle with an arbitrary shape is equivalent to a suitably chosen general ellipsoid of the same volume, as far as the total energy is concerned. In all the sequel, we shall assume that the particle under study is spherical and single-domain.

## 2.1 Magnetization switching under magnetic field: Stoner-Wohlfarth model

In small magnetic particles exchange interaction may be strong enough to hold all spins tightly parallel to each other, and prevents spatial dependence of the particle's magnetization. We have shown [7], [9] that this no longer holds when free-boundary effects and/or surface anisotropy are taken into consideration. Ignoring surface effects, or in other words spatial inhomogeneities, the exchange energy is a constant and plays no role in the energy minimization. In the latter only the anisotropy energy and the interaction with the applied field are relevant. Accordingly, let us consider the simplest case of a magnetic moment  $\mathbf{m}$  with a uniaxial anisotropy axis  $\mathbf{e}$  along the  $z$  direction of the applied field. The corresponding Hamiltonian reads

$$\mathcal{H} = -\frac{Kv}{m^2}(\mathbf{m} \cdot \mathbf{e})^2 - \mathbf{m} \cdot \mathbf{H}, \quad (1)$$

where  $K$  is the magneto-crystalline anisotropy constant and  $v$  is the volume of the particle. Upon writing  $\mathbf{m} = m\mathbf{s}$ ,  $\mathbf{H} = H\mathbf{e}_h$ , and introducing the dimensionless anisotropy and field parameters

$$\sigma = \frac{Kv}{k_B T}, \quad h = \frac{Hm}{2Kv}, \quad (2)$$

where  $k_B$  is the Boltzmann constant, the Hamiltonian (1), divided by thermal energy, becomes

$$-\beta\mathcal{H} = \sigma \left[ (\mathbf{s} \cdot \mathbf{e})^2 + 2h(\mathbf{s} \cdot \mathbf{e}_h) \right]. \quad (3)$$

Denoting by  $\theta$  the angle between the magnetization direction  $\mathbf{s}$  and the field direction  $\mathbf{e}_h$ , we write (3) as

$$-\beta\mathcal{H} = \sigma \left[ \cos^2 \theta + 2h \cos \theta \right]. \quad (4)$$

For simplicity, we only consider the case of easy axis, i.e.,  $\sigma < 0$ . For  $\sigma > 0$  (easy plane) the results are the same only that the energy maximum and minimum are interchanged. The extrema of  $\mathcal{H}$  and their nature are obtained by setting to zero its first derivative with respect to  $\theta$ , and evaluating the second derivative at these extrema. The results are presented in Table 1. Thus, for  $|h| < 1$  the energy has minima at  $\theta = 0$  and  $\theta = \pi$ , separated by a maximum at  $\theta_m = \arccos(-h)$ . For  $|h| \gtrsim 1$  the upper (also the shallower) energy minimum ( $\theta = \pi$  for  $h > 0$ ) turns into a maximum as it merges with the intermediate maximum at  $\theta_m$ , which disappears (see Fig. 1). From the values of the energy

Table 1

Field	Minima	Maxima
$ h  < 1$	$\theta = 0, \pi$	$\theta = \arccos(-h)$
$h > 1$	$\theta = 0$	$\theta = \pi$
$h < -1$	$\theta = \pi$	$\theta = 0$

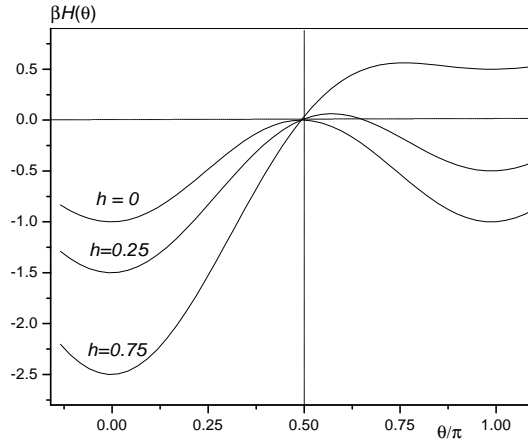


Fig. 1. Magnetic energy in the case of longitudinal field for some values of the reduced field  $h$ . Upon increasing the field the number of potential wells changes from two to one.

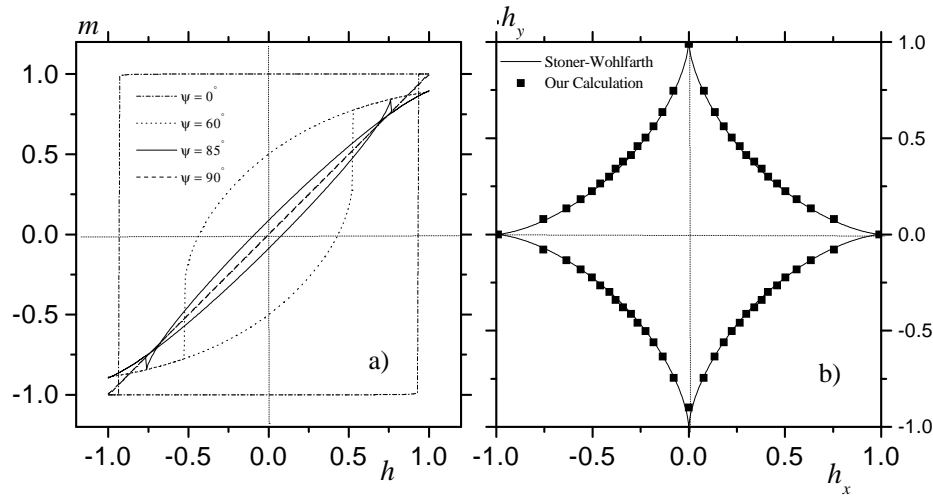


Fig. 2. Left: (numerical) hysteresis loops for different values of  $\psi$  increasing inwards:  $\psi = 0^\circ, 60^\circ, 85^\circ, 90^\circ$ , for a  $3^3$  particle with uniaxial anisotropy and strong exchange coupling. Right: (numerical in squares and analytical in full line) SW astroid for the same particle.

at  $\theta = 0, \pi$  and, when it exists, at the intermediate maximum  $\theta_m$ , one obtains the energy-barrier heights ( $|h| < 1$ )

$$\Delta\mathcal{H} = \beta [\mathcal{H}(\theta_m) - \mathcal{H}(0, \pi)] = \sigma(1 \pm h)^2. \quad (5)$$

The analysis above helps solve for the hysteresis curve, an important part of magnetism, for small ferromagnetic particles. Such calculations are known as the Stoner-Wohlfarth model [5]. In their original study, Stoner and Wohlfarth considered shape anisotropy instead of uniaxial anisotropy. However, their model is usually applied to the latter. In addition, they also considered the more general situation of a field applied at an arbitrary angle  $\psi$  to the easy axis. From the above analysis we see that there is a unique minimum for  $|h| > 1$  while there are two minima for  $|h| < 1$ . This is due to the multivaluedness of the trigonometric functions entering the Hamiltonian (4) and its derivatives with respect to  $\theta$ . In order to obtain a unique solution, one has to specify and follow the history of the field  $h$  for each angle  $\psi$ . One usually starts at saturation and increases (or decreases) the field across zero until it reaches the value at which the energy barrier disappears. This field marks the *limit of metastability* and is called the *critical field*. In Stoner-Wohlfarth model, this is given by  $|h| = 1$  [for  $\psi = 0$ ]. For arbitrary  $\psi$  the critical field is given by

$$h_c = \frac{1}{\left(\cos^{2/3} \psi + \sin^{2/3} \psi\right)^{3/2}}.$$

One can also define what is called the *switching field*, that is the field at which the magnetization changes sign.

In Fig. 2 we present (on the left) the hysteresis loop at different angles  $\psi$ , and on the right (in full line) the angular dependence of the switching field, the so-called Stoner-Wohlfarth astroid, as obtained from the Stoner-Wohlfarth model [see Eq. (15) with  $a = 0$ ]. In fact, the hysteresis loops in Fig. 2 and the astroid in squares, were obtained from the numerical solution of the Landau-Lifshitz equation [9].

Stoner-Wohlfarth astroids for cubic anisotropy have been obtained by Thiaville [10] using a geometrical approach.

## 2.2 Thermal effects on the Stoner-Wohlfarth model: Landau theory

Before dealing with the effect of thermoactivation on the magnetization switching between the different energy minima, and discuss the calculation of the corresponding relaxation time, we now consider the effect of temperature on the Stoner-Wohlfarth model [7]. More precisely, we consider magnetization

switching at a long-time scale, i.e., at quasi-equilibrium. In [7] we derived a free energy for weakly anisotropic ferromagnets which is valid in the whole range of temperature and interpolates between the micromagnetic energy at zero temperature and the Landau free energy near the Curie point  $T_c$ . This free energy takes into account the change of the magnetization magnitude due to thermal effects, in particular, in the inhomogeneous states. As an illustration, we studied the thermal effect on the Stoner-Wohlfarth astroid and hysteresis loop of a ferromagnetic nanoparticle assuming that it is in a single-domain state. Within this model, the saddle point of the particle's free energy, as well as the metastability boundary, are due to the change in the magnetization magnitude sufficiently close to  $T_c$ , as opposed to the usual homogeneous rotation process at lower temperatures.

For weakly anisotropic magnets, where the anisotropy energy is much weaker than the homogeneous exchange energy, the magnetization magnitude  $M$  is either small or only slightly deviates from  $M_e$ , the equilibrium magnetization at zero field. Thus the condition for the magnetization minimizing the free energy derived in [7],  $|M - M_e| \ll M_s$ , where  $M_s$  is the saturation magnetization at  $T = 0$ , is satisfied in the whole temperature range. In [7] we presented the derivation of this free energy and illustrated some of its features in the case of a single-domain magnetic particle with a uniaxial anisotropy.

For single-domain magnetic particles in a homogeneous state, the gradient (exchange) terms in the free energy can be dropped and the free energy can be written in the form

$$F = F_e + (VM_e^2/\chi_\perp)f$$

$$f = -\mathbf{n} \cdot \mathbf{h} + \frac{1}{2}(n_x^2 + n_y^2) + \frac{1}{4a}(n^2 - 1)^2, \quad (6)$$

where  $V$  is the particle's volume and  $f$  the reduced free energy in terms of the reduced variables

$$\mathbf{n} \equiv \mathbf{M}/M_e, \quad \mathbf{h} \equiv \mathbf{H}\chi_\perp/M_e, \quad a \equiv 2\chi_\parallel/\chi_\perp. \quad (7)$$

where  $\chi_\parallel/$  and  $\chi_\perp$  are the longitudinal and transverse susceptibilities. We see that the parameter  $a$  here controls the rigidity of the magnetization vector; it goes to zero in the zero-temperature limit (with fixed magnetization modulus) and diverges at  $T_c$ .

For fields  $\mathbf{h}$  inside the Stoner-Wohlfarth astroid [see Fig. 2 (right)], which will be generalized here to nonzero temperatures,  $f$  has two minima separated by a barrier. Owing to the axial symmetry, one can set  $n_y = 0$  for the investigation of the free energy scape. The minima, saddle points, and the maximum can be found from the equations  $\partial f/\partial n_x = \partial f/\partial n_z = 0$ , or, explicitly



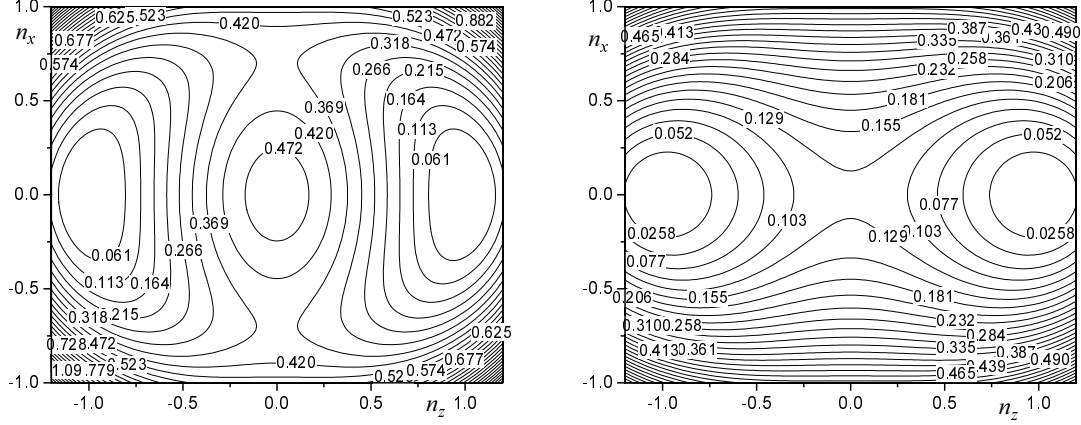


Fig. 3. The free energy of a ferromagnetic particle with uniaxial anisotropy [ $f$  in Eq. (6) in zero field] for  $a \equiv 2\chi_{\parallel}/\chi_{\perp} = 0.5$  (left) and  $a = 2$  (right) corresponding to lower and higher temperatures, respectively.

$$\begin{aligned} n_z(n^2 - 1) &= ah_z \\ n_x(n^2 - 1 + a) &= ah_x. \end{aligned} \quad (8)$$

Solving for  $n_x$  one obtains a 5th-order equation for  $n_z$

$$h_x^2 n_z^3 = (h_z + n_z)^2 (ah_z + n_z - n_z^3). \quad (9)$$

In zero field, the characteristic points of the energyscape can be simply found from Eqs. (8). One of these points is  $n_x = n_z = 0$ , which is a local maximum for  $a < 1$  and a saddle point for  $a > 1$ . The minima are given by  $n_x = 0$ ,  $n_z = \pm 1$ . The saddle points correspond to  $n_z = 0$ , while from the second of Eqs. (8) one finds

$$n_x = \begin{cases} \pm\sqrt{1-a}, & a \leq 1 \\ 0, & a \geq 1. \end{cases} \quad (10)$$

In fact, due to the axial symmetry, for  $a < 1$  one has a saddle circle  $n_x^2 + n_y^2 = 1 - a$ , rather than two saddle points. The free-energy barrier following from this solution is given by

$$\Delta f \equiv f_{\text{sad}} - f_{\text{min}} = \begin{cases} (2-a)/4, & a \leq 1 \\ 1/(4a), & a \geq 1. \end{cases} \quad (11)$$

The free-energy landscape in zero field is shown in Fig. 3. At nonzero temperatures  $a > 0$ , the magnitude of the magnetization at the saddle is smaller

than unity since it is directed perpendicular to the easy axis, and for this orientation the “equilibrium” magnetization is smaller than in the direction along the  $z$  axis. For  $a > 1$ , the two saddle points, or rather the saddle circle, degenerate into a single saddle point at  $n_x = n_z = 0$ , and the local maximum there disappears. That is, for the magnetization to overcome the barrier, it is easier to change its magnitude than its direction. This is a phenomenon of the same kind as the phase transition in ferromagnets between the Ising-like domain walls in the vicinity of  $T_c$  (the magnetization changes its magnitude and is everywhere directed along the  $z$  axis) and the Bloch walls at lower temperatures [11], [12].

The Stoner-Wohlfarth curve separates the regions where there are two minima and one minimum of the free energy. On this curve the metastable minimum merges with the saddle point and loses its local stability. The corresponding condition is

$$\partial^2 f / \partial n_x^2 \times \partial^2 f / \partial n_z^2 - (\partial^2 f / \partial n_x \partial n_z)^2 = 0, \quad (12)$$

which upon using Eq. (9) leads to the quartic equation for  $n_z$

$$h_z[(2 + a)n_z + 3ah_z] + 2n_z^4 = 0. \quad (13)$$

Before considering the general case, let us analyze the limiting cases  $a \ll 1$  and  $a \gg 1$ .

At low temperatures, i.e.,  $a \ll 1$ , the magnetization only slightly deviates from its equilibrium value, and to first order in  $a$ , one obtains

$$n^2 \cong 1 - an_z^2 \quad \text{or} \quad n_x^2 + (1 + a)n_z^2 \cong 1. \quad (14)$$

From Eq. (13) and the analogous equation for  $n_x$  one derives the equation for the Stoner-Wohlfarth astroid

$$h_x^{2/3} + [(1 + a/2)h_z]^{2/3} \cong 1, \quad a \ll 1. \quad (15)$$

One can see that, in comparison with the standard zero-temperature Stoner-Wohlfarth astroid, i.e. at  $a = 0$ ,  $h_z$  is rescaled. The critical field in the  $z$  direction decreases because of the field dependence of the magnetization magnitude at nonzero temperatures.

Similarly, in the case  $a \gg 1$ , i.e. near  $T_c$ , Eq. (12) leads to the equation for Stoner-Wohlfarth curve

$$n_x^2 + 3n_z^2 \cong 1. \quad (16)$$

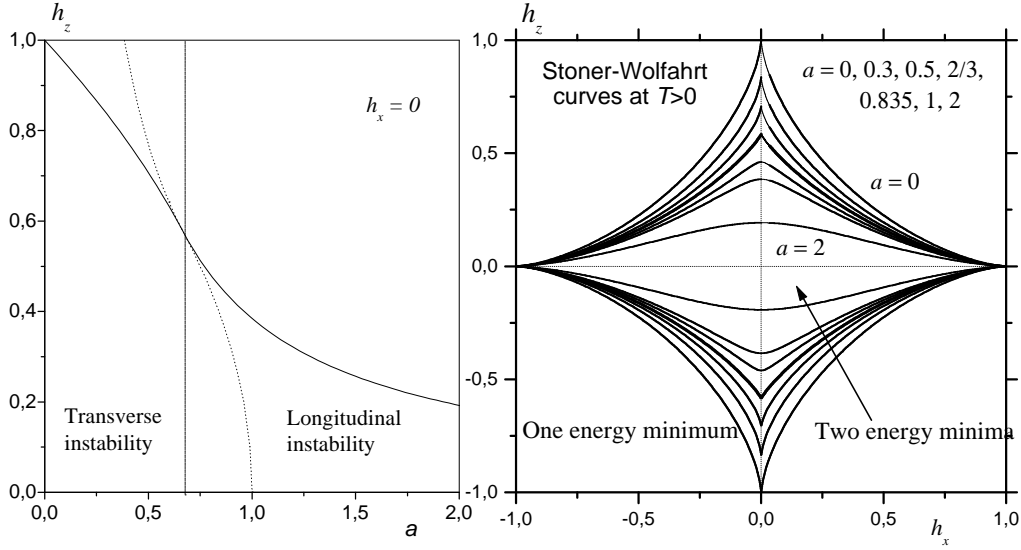


Fig. 4. Left: Dependence  $h_z(a)$  at  $h_x = 0$  on the Stoner-Wohlfarth curve. Right: The Stoner-Wohlfarth curves at different temperatures,  $a \equiv 2\chi_{\parallel}/\chi_{\perp} = 0$  ( $T = 0$ ), 0.3, 0.5,  $2/3$ , 0.835, 1, 2.

and upon using Eq. (8) we infer

$$n_z \cong -(ah_z/2)^{1/3}, \quad n_x \cong h_x. \quad (17)$$

Making use of this result in Eq. (16), one obtains another limiting case of the Stoner-Wohlfarth curve

$$h_x^2 + 3(ah_z/2)^{2/3} \cong 1, \quad a \gg 1. \quad (18)$$

In this case, the critical field (i.e., the field on the Stoner-Wohlfarth curve) in the  $z$  direction is strongly reduced, and there is no singularity in the dependence  $h_{cz}(h_x)$  at  $h_x = 0$ .

The qualitatively different character of the Stoner-Wohlfarth curves in these two cases is due to the different mechanisms pertaining to the loss of the local stability for the field applied along the  $z$  axis. For  $h_x = 0$  the mixed derivative  $(\partial^2 f / \partial n_x \partial n_z)$  vanishes and Eq. (12) factorizes,

$$(a - 1 + n_z^2)(-1 + 3n_z^2) = 0. \quad (19)$$

Vanishing of the first factor in this equation corresponds to the loss of stability with respect to the rotation of the magnetization,  $\partial^2 f / \partial n_x^2 = 0$ , and vanishing of the second factor,  $\partial^2 f / \partial n_z^2 = 0$ , implies the loss of stability with respect to

the change of the magnetization magnitude. Using  $n_x = 0$ , with the help of the first equality in Eq. (9) one obtains in the two cases

$$h_{cz} = \begin{cases} h_{z\parallel} \equiv \sqrt{1-a}, & a \leq 2/3 \\ h_{z\perp} \equiv 2/(3^{3/2}a), & a \geq 2/3. \end{cases} \quad (20)$$

Note that the transition between the two regimes occurs here at a different value of  $a$  than in Eq. (10). The dependence  $h_z(a)$  at  $h_x = 0$  is shown in Fig. 4 (left).

In the general case, it is easier to find the Stoner-Wohlfarth curve numerically from Eqs. (8) and (13). The results in the whole range of  $a$  are shown in Fig. 4 (right).

We have shown that, for single-domain magnetic particles with uniaxial anisotropy, thermal effects qualitatively change the free-energy landscape at sufficiently high temperatures, so that the passage from one free-energy minimum to the other is realized by the *uniform change of the magnetization magnitude* rather than the *uniform rotation*. This also qualitatively changes the character of the Stoner-Wohlfarth curve and hysteresis loops [7]. These effects cannot be observed with standard methods, however, because keeping the height of the free-energy barrier much larger than thermal energy requires so large particle sizes that the single-domain criterion is no longer satisfied [see discussion in Sect. 6 of Ref.[7]]. For the uniform states, the theory is valid at low temperatures, but then the thermal effects considered here are small corrections to the zero-temperature results.

Finally, we would like to mention that quite recently, experimental results have been obtained by Jamet et al. [13] on 3 nm cobalt nanoparticles which clearly show the disappearance of the singularity near  $H_x = 0$  at a temperature circa 8 K (the blocking temperature being 14 K). The height of the experimental astroid decreases nearly as its width with increasing temperature, but it does not become flat as predicted by our calculations. This failure of our theory, in addition to the fact that this effect is predicted at much higher temperatures, is not surprising considering the fact that  $T \ll T_c$ . Nevertheless, the disappearance of the singularity is definitely predicted by our theory.

### 2.3 Magnetization switching as a thermal effect: Néel-Brown model

We have seen that the Stoner-Wohlfarth model accounts for the hysteretic rotation of the particle's magnetization over the potential barrier under the influence of a field applied in an arbitrary direction, at zero temperature.

We also considered the effect of temperature on the Stoner-Wohlfarth model but at quasi-equilibrium. Now, we come to deal with the thermoactivated switching of the particle's magnetic moment, a process that occurs at short-time scales. At nonzero temperatures the magnetization vector of the particle can surmount the energy barrier due to thermal fluctuations as argued by Néel [1]. This effect is particularly pronounced for small particles with lower values of the potential barrier (5). Indeed, the magnetization vector of the particle shuttles between the two energy minima and the characteristic time for this thermoactivated rotation of the spin over the anisotropy barrier  $\Delta\mathcal{H}$  is approximately given by the celebrated Van't Hoff-Arrhenius law [14], [15]

$$\tau = \tau_0 e^{\Delta\mathcal{H}/k_B T}, \quad (21)$$

where  $\tau_0$  is usually taken as temperature and field independent and on the order of  $10^{-10} - 10^{-12}$ s.  $\tau_0$  is not necessarily the same for different ferromagnetic materials. It can indeed be assumed as constant only if the magnetization vector is always in one of the energy minima, which happens only if the minima have zero width, or equivalently if the barrier is infinitely high. However, in any realistic case, there is a finite probability that the magnetization vector spends some time in the vicinity of either minimum, in which case the prefactor need not be constant, and certainly depends on temperature and field. Indeed, in the case of cubic anisotropy the assumption of a constant prefactor  $\tau_0$  turns out to be a bad approximation [16]. For a given measuring time  $\tau_m$  the system is at thermal equilibrium when  $\tau_m \gg \tau$ , and in this case the particle is said to be *superparamagnetic*, which corresponds to the temperature range

$$\ln(\tau_m/\tau_0) > \Delta\mathcal{H}/k_B T \geq 0. \quad (22)$$

In fact, it was argued in [17] that due to the smallness of  $\tau_0$  the range of thermal equilibrium can extend down to temperatures at which the energy-barrier height is much larger than thermal energy. More precisely, for magnetic measurements with  $\tau_m \sim 100$ s, this range is  $0 \leq \Delta\mathcal{H}/k_B T < 25$ , which means that it is too restrictive to argue that superparamagnetism occurs only when thermal energy is on the order of the energy-barrier height. In the case  $\tau \gg \tau_m$  the particle's magnetization does not change during the time of observation, and the particle exhibits stable ferromagnetism and is said to be in a *blocked state*. The temperature at which such a transition occurs, namely the temperature at which the relaxation time  $\tau$  is equal to the observation time  $\tau_m$ , is called the *blocking temperature* and is denoted by  $T_B$ . For nanoparticle assemblies with size distribution, the same temperature may sometimes be above  $T_B$  for some particles, and below it for the others. Such systems may thus behave as superparamagnetic for some high values of the temperature  $T$ , as ferromagnetic at low values of  $T$ , and as a mixture of both at intermediate  $T$ . For such a system

a different characteristic temperature is used, this is denoted by  $T_{\max}$ , and is roughly given, at least in the dilute case, by an average of all  $T_B$ 's. One should not forget however that the scale of 100s depends on the experimental apparatus. Indeed, in Mössbauer effect measurements, the experimental time is the time of Larmor precession, which is on the order of  $10^{-8}$ s, while in neutron scattering experiments it is on the order of  $10^{-12}$ s. In addition, the time scale can be completely different in different areas of applications. For example, in magnetic recording, in order to keep the data stored on a magnetic tape for years, one should have  $\tau \gg 10^8$ s, and in rock magnetism the magnetization decays (or relaxes) within geological times which may be millions of years.

Owing to these important practical applications and many others, the relaxation time of the particle's magnetization is a very important and fundamental physical quantity that deserves extensive and rigorous investigation. This actually started, in this context, with the work of Kramers on transition-state method [18]. Kramers showed, by using the theory of the Brownian motion, how the prefactor of the reaction rate (inverse of relaxation time), as a function of the damping parameter and the shape of the potential well, could be calculated from the underlying probability-density diffusion equation in phase space, which for Brownian motion is the Fokker-Planck equation (FPE). He obtained, by linearizing the FPE about the potential barrier, explicit results for the escape rate for intermediate-to-high (IHD) values of the damping parameter and also for very small values of that parameter. Subsequently, a number of authors [19], [20] showed how this approach could be extended to give formulae for the reaction rate which are valid for all values of the damping parameter. These calculations have been reviewed by Hänggi et al. [21].

Kramers theory, originally developed for mechanical particles, was first adapted to the thermal rotational motion of the magnetic moment by Brown [2] in order to improve upon Néel's concept of the superparamagnetic relaxation process, which implicitly assumes discrete orientations of the magnetic moment and which does not take into account the gyromagnetic nature of the system. Brown in his first explicit calculation [2] of the escape rate confined himself to axially symmetric (functions of the latitude only) potentials of the magneto-crystalline anisotropy so that the calculation of the relaxation rate is governed [for potential-barrier height significantly greater than  $k_B T$ ] by the smallest non-vanishing eigenvalue  $\lambda_1$  of the Sturm-Liouville equation associated with the one-dimensional FPE. Thus the rate obtained is valid for all values of the damping parameter. As a consequence of this very particular result, the analogy with the Kramers theory for mechanical particles only becomes fully apparent when an attempt is made to treat non axially symmetric potentials of the magneto-crystalline anisotropy that are functions of both the latitude and the longitude. In this context, Brown [2] succeeded in giving a formula for the escape rate for magnetic moments of single-domain particles, in the IHD damping limit, which is the analog of the Kramers IHD

formula for mechanical particles. In his second 1979 calculation [3] Brown only considered this case. Later Klik and Gunther [22], by using the theory of first-passage times, obtained a formula for the escape rate which is the analog of the Kramers result for very low damping. All these (asymptotic) formulae which apply to a general non-axially symmetric potential, were calculated explicitly for the case of a uniform magnetic field applied at an arbitrary angle to the anisotropy axis of the particle by Geoghegan et al. [23] and compare favorably with the exact reaction rate given by the smallest non-vanishing eigenvalue of the FPE [24], [25], [26], [27] and with experiments on the relaxation time of single-domain particles [26], [28].

In both limiting cases considered by Brown the time dependence of the average magnetization is a single exponential and the relaxation rate is given by the eigenvalue  $\lambda_1$  previously mentioned. Subsequently,  $\lambda_1$  was numerically calculated by Aharoni for arbitrary values of  $\Delta\mathcal{H}/k_B T$  without a magnetic field [29] and in a longitudinal magnetic field [30]. The correction terms for the high-barrier result for  $\lambda_1$  were given by Brown [31]. Various limiting cases and the corresponding expressions for  $\lambda_1$  were further investigated in [32], [33], [34], [35], [24]. Let aside such limiting cases, the FPE for an assembly of single-domain ferromagnetic particles cannot be solved analytically. The magnetization relaxation curve in fact consists of an infinite number of exponentials. In this case, it was shown in Refs. [36], [37], [38] that it is more convenient to introduce the so-called *integral relaxation time*  $\tau_{int}$ , defined as the area under the relaxation curve after a sudden infinitesimal change of the magnetic field.  $\tau_{int}$  depends on all eigenvalues  $\lambda_k, k = 1, 2, \dots$  and therefore contains more information than can be rendered by the first eigenvalue  $\lambda_1$ , and more importantly, it can be measured experimentally. Moreover, it turns out that, unlike  $\lambda_1$ ,  $\tau_{int}$  can be calculated analytically for uniaxial particles in the longitudinal magnetic field for the arbitrary values of the damping parameter, and  $\tau_{int}^{-1}$  recovers the analytical results of Brown for  $\lambda_1$  in the asymptotic regions. It was shown in [37] that the drastic deviation of  $\tau_{int}^{-1}$  from  $\lambda_1$  at low temperatures, starting from some critical value of the field, is a consequence of the depletion of the upper potential well. In these conditions, the integral relaxation time  $\tau_{int}$  consists of two competing contributions corresponding to the overbarrier and intrawell relaxation processes.

After the above survey, we now give some of the most commonly used expressions for the relaxation time, together with some cautionary remarks. As indicated above, Brown [2] at first derived a formula for  $\lambda_1$ , for an arbitrary *axially symmetric* bistable potential of Fig. 1 with minima at  $\theta = (0, \pi)$  separated by a maximum at  $\theta_m = \arccos(-h)$ , which when applied to Eq. (3) for  $\mathbf{h} \parallel \mathbf{e}$ , i.e. a magnetic field parallel to the easy axis, leads to the form given by

Aharoni [30],

$$\lambda_1 \simeq \frac{2\alpha\gamma K^{3/2}}{m} \sqrt{\frac{\beta}{\pi}} (1-h^2) \times \left[ (1+h) e^{-\beta K(1+h)^2} + (1-h) e^{-\beta K(1-h)^2} \right], \quad (23)$$

where  $\gamma$  is the gyromagnetic factor,  $\alpha$  the damping parameter.  $0 \leq h \leq 1$ ,  $h = 1$  being the critical value at which the bistable nature of the potential disappears [see section 2.1].

In order to describe the non-axially symmetric asymptotic behavior, let us denote by  $\beta\Delta\mathcal{H}_-$  the smaller reduced barrier height of the two constituting escape from the left or the right of a bistable potential [see Eq. (5) for the axially-symmetric case]. Then for very low damping, i.e. for  $\alpha \times \beta\Delta\mathcal{H}_- \ll 1$  (with of course the reduced barrier height  $\beta\Delta\mathcal{H}_- \gg 1$ , depending on the size of the nanoparticle), we have [2], [27] the following asymptotic expression for the inverse relaxation time

$$\begin{aligned} \tau_{VLD}^{-1} &\simeq \frac{\lambda}{2\tau_N} \\ &\simeq \frac{\alpha}{2\pi} \left\{ \omega_1 \times \beta(\mathcal{H}_0 - \mathcal{H}_1) e^{-\beta(\mathcal{H}_0 - \mathcal{H}_1)} + \omega_2 \times \beta(\mathcal{H}_0 - \mathcal{H}_2) e^{-\beta(\mathcal{H}_0 - \mathcal{H}_2)} \right\}, \end{aligned} \quad (24)$$

where  $\alpha$  is the damping parameter and

$$\tau_N = \frac{1}{\alpha} \frac{\beta m}{2\gamma}, \quad (25)$$

is the free-diffusion time, i.e., the characteristic time of diffusion in the absence of the potential. For the IHD limit, where  $\alpha \times \beta\Delta\mathcal{H}_- > 1$  (again with the reduced barrier height  $\beta\Delta\mathcal{H}_-$  much greater than unity) we have [27] the asymptotic expression

$$\tau_{IHD}^{-1} \simeq \frac{\Omega_0}{2\pi\omega_0} \left\{ \omega_1 e^{-\beta(\mathcal{H}_0 - \mathcal{H}_1)} + \omega_2 e^{-\beta(\mathcal{H}_0 - \mathcal{H}_2)} \right\}, \quad (26)$$

where

$$\begin{aligned} \omega_1^2 &= \frac{\gamma^2}{m^2} c_1^{(1)} c_2^{(1)}, \quad \omega_2^2 = \frac{\gamma^2}{m^2} c_1^{(2)} c_2^{(2)}, \quad \omega_0^2 = -\frac{\gamma^2}{m^2} c_1^{(0)} c_2^{(0)}, \\ \Omega_0 &= \frac{\alpha\gamma}{2m} \left[ -c_1^{(0)} - c_2^{(0)} + \sqrt{(c_2^{(0)} - c_1^{(0)})^2 - 4c_1^{(0)} c_2^{(0)}} \right]. \end{aligned}$$

Here  $\omega_1, \omega_2$  and  $\omega_0$  are respectively the wells and saddle angular frequencies associated with the bistable potential,  $\Omega_0$  is the damped saddle angular frequency and the  $c_j^{(i)}$  are the coefficients of the truncated (at the second order



in the direction cosines) Taylor series expansion of the crystalline anisotropy and external field potential at the wells of the bistable potential denoted by 1 and 2 and at the saddle point denoted by 0. A full discussion of the application of these general formulae to the particular potential, which involves the numerical solution of a quartic equation in order to determine the  $c_j^{(i)}$  with the exception of the particular field angle  $\psi = \frac{\pi}{4}$  or  $\frac{\pi}{2}$ , in Eq.(1) is given in Refs. [23], [39].

In Ref. [40], we used either Eqs. (23) and (24) or (23) and (26), and solved the equation  $\tau = \tau_m$  for the blocking temperature  $T_B$ , as a function of the applied field, for an arbitrary angle  $\psi$  between the easy axis and the applied magnetic field. In particular, for very small values of  $\psi$  we used Eq. (23), as the problem then becomes almost axially symmetric and the arguments leading to Eqs. (24) and (26) fail [2], [3], [23], and appropriate connection formulae had to be used so that they may attain the axially symmetric limit. Application of the above asymptotic formulae to the calculation of the blocking temperature  $T_B$  (or  $T_{\max}$ ) as a function of the applied field appeared to recover the experimental observation, but this result turned out to be spurious. An explanation of this behavior follows (see also [41], [42]): in the non-axially symmetric IHD asymptote (26), which is formulated in terms of the Kramers escape rate, as the field tends to zero, for high damping, the saddle angular frequency  $\omega_0$  tends to zero. Thus the saddle becomes infinitely wide and so the escape rate predicted by Eq. (26) diverges [see similar discussion in Sect. 3] leading to an apparent rise in the blocking temperature until the field reaches a value sufficiently high to allow the exponential in the Arrhenius terms to take over. When this occurs the blocking temperature decreases again in accordance with the expected behavior. This is the field range where one would expect the non-axially asymptote to work well. In reality, as demonstrated by exact numerical calculations of the smallest non vanishing eigenvalue of the Fokker-Planck matrix, the small field behavior is not as predicted by the asymptotic behavior of Eq. (26) (it is rather given by the axially-symmetric asymptote) because the saddle is limited in size to  $\omega_0$ . Thus the true escape rate cannot diverge, and the apparent discontinuity between the axially-symmetric and non axially-symmetric results is spurious, leading to an apparent maximum in  $T_B(h)$ . In reality, the prefactor in Eq. (26) can never overcome the exponential decrease embodied in the Arrhenius factor. Garanin [41] has discovered bridging formulae which provide continuity between the axially-symmetric Eq. (23) and non-axially symmetric asymptotes leading to a monotonic decrease of the blocking temperature with the field in accordance with the numerical calculations of the lowest eigenvalue of the Fokker-Planck equation and also in agreement with the fact that the field suppresses the energy barrier upon which the blocking temperature decreases.

An illustration of this was given in Ref. [41] [see also [42] for more detail] for the particular case of  $\psi = \pi/2$ , that is a transverse field. If the escape rate is

written in the form

$$\tau^{-1} = \frac{\kappa}{\pi} A \exp(-\beta \Delta \mathcal{H})$$

where  $\kappa$  is the attempt frequency given by

$$\kappa = \frac{2K\gamma}{m} \sqrt{1 - h^2},$$

then the factor  $A$ , as predicted by the IHD formula, behaves as  $\alpha/\sqrt{h}$  for  $h \ll 1, \alpha^2$ , while for  $h = 0$ ,  $A$  behaves as  $2\pi\alpha\sqrt{\sigma/\pi}$ , which is obviously discontinuous. So, a suitable interpolation formula is required. Such a formula (analogous to that used in the WKBJ method [43]) is obtained by multiplying the factor  $A$  of the axially symmetric result by  $e^{-\xi} I_0(\xi)$ , where  $I_0(\xi)$  is the modified Bessel function of the first kind, and  $\xi = 2\sigma h$  [see [41]]. This interpolation formula, as is obvious from the large and small  $\xi$  limits, automatically removes the undesirable  $1/\sqrt{h}$  divergence of the IHD formula and establishes continuity between the axially symmetric and non-axially symmetric asymptotes for  $\psi = \pi/2$ , as dictated by the exact solution.

It is apparent from the discussion of this section that the Néel-Brown model for a single particle is unable to explain the maximum in  $T_{\max}$ , observed in experiments, as a careful calculation of the asymptotes demonstrates that they always predict a monotonic decrease in the blocking temperature. A possible explanation of the maximum of  $T_{\max}$  as a function of the applied field was given in [40] where it was shown that the non-linearity of the field dependence of the superparamagnetic contribution to the assembly magnetization, volume distribution, and anisotropy are responsible for this effect.

### 3 A first step beyond the Néel-Brown model: effect of exchange interaction

As discussed in the introduction, in order to calculate the relaxation time of a nanoparticle in an inhomogeneous magnetic state induced by surface effects, one has to resort to microscopic theories. Then, one has to take account explicitly of microscopic interactions, such as exchange and/or dipolar interactions, in addition to the magneto-crystalline and surface anisotropy and applied magnetic field. However, the problem associated with the generalization of Brown's theory to include interactions and eventually surface effects is really involved and can in general only be tackled numerically. But before one can attack this problem, one needs to understand the effect of, e.g., exchange interaction on the relaxation time of the minimal system, i.e., a pair of atomic spins coupled via exchange interaction, including of course the usual magneto-crystalline anisotropy and Zeeman terms. Besides, this is the unique

non-trivial step towards the above-mentioned generalization, where analytical expressions can be obtained for the relaxation time. It was the purpose of Ref. [44] to solve this problem and to compare with the Néel-Brown result in the one-spin approximation. Accordingly, we studied the effect of exchange coupling on the relaxation rate of a magnetic system of two spins within Langer’s approach. We found a particular value of the exchange coupling, that is  $j \equiv J/K = j_c \equiv 1 - h^2$ , where  $h \equiv H/2K$ , at which the number of saddle points changes. For  $j \leq j_c$  there are two saddle points and the reversal of the spins proceeds in two steps: the first spin crosses one of the saddle points into the anti-ferromagnetic state, and then the other spin follows across the second saddle point, to end up in the ferromagnetic order of opposite direction with respect to the initial one. For  $j > j_c$ , the two spins are so strongly exchange-coupled that they cross a single saddle point together. For  $j \gg j_c$  the Néel-Brown result for a single spin is recovered. As a byproduct, we also showed that Langer’s quadratic approximation of the potential energy at the saddle point fails when the exchange coupling assumes the critical value  $j_c$  even in the IHD limit.

It is worth mentioning that the effect of dipolar interactions on the relaxation time of magnetic systems has been studied by a few authors. In Ref. [45], [46] this was done for assemblies of nanoparticles where approximate expressions were obtained using the (mean-field) barrier-height approach that is only valid in the limit of infinite damping (no gyromagnetic effect). In Ref. [47] the authors used perturbation theory and obtained an expression for the relaxation rate in the case of weakly interacting superparamagnets with various anisotropy orientations and in the absence of external field. Finally, the authors of Ref. [48] dealt with a pair of coupled dipoles using the (numerical) Langevin approach and found some results similar to ours [see below].

In this section we will first give a brief account of Langer’s approach [49] (see also [51] for uniform (one-spin problem) and non-uniform magnetization and [52] for comparison with Kramers’ theory).

### 3.1 Switching rate in Langer’s approach

Within this approach the problem of calculating the relaxation time for a multidimensional process is reduced to solving a steady-state equation in the immediate neighborhood of the saddle point that the system crosses as it goes from a metastable state to another state of greater stability. The basic idea [49] is that “... *one imagines setting up a steady-state situation by continuously replenishing the metastable state at a rate equal to the rate at which it is leaking across the activation-energy barrier. By identifying the current flowing over the barrier with the desired decay rate, one avoids having to solve the complete*

*time-dependent problem...*”, especially in the multidimensional case where this problem is too difficult to solve. However, this approach is only valid in the limit of intermediate-to-high damping because of the assumption, inherent to this approach, that the potential energy in the vicinity of the saddle point may be approximated by its second-order Taylor expansion (see below). The result for small damping fails because the region of deviation from the Maxwell-Boltzmann distribution, set up in the well, extends far beyond the narrow region at the top of the barrier in which the potential may be replaced by its quadratic approximation. Therefore, in Langer’s approach, one concentrates on the distribution function  $\rho(\{\eta\}, t)$  as the probability that the system is found in the configuration  $\{\eta\}$  at time  $t$ . The time evolution of  $\rho$  is governed by the following equation

$$\frac{\partial \rho}{\partial t} = \left( \frac{\partial \rho}{\partial t} \right)_{dyn.} + \left( \frac{\partial \rho}{\partial t} \right)_{fluct.} \quad (27)$$

where the first term accounts for the “internal” dynamics of the system described by

$$\frac{\partial \eta_i}{\partial t} = \sum_j A_{ij} \frac{\partial \mathcal{H}}{\partial \eta_j}, \quad (28)$$

where  $A$  is a fully anti-symmetric matrix. For a magnetic system, as in our case, the analog of Eq. (28) is given by the Landau-Lifshitz equations (50). The second term in (27) accounts for the dynamics of the system driven by its interaction with the heat bath, and is given by [49]

$$\left( \frac{\partial \rho}{\partial t} \right)_{fluct.} = \sum_i \Gamma_i \frac{\partial}{\partial \eta_i} \left( \beta \frac{\partial \mathcal{H}}{\partial \eta_i} + \frac{\partial \rho}{\partial \eta_i} \right). \quad (29)$$

where  $\beta = 1/k_B T$  and the constant  $\Gamma_i$  characterizes the variation rate of  $\eta_i(t)$ . Combining Eqs. (28) and (29) in Eq. (27) leads to the Fokker-Planck equation

$$\partial_t \rho + \sum_i \partial_{\eta_i} J_i = 0, \quad (30)$$

which is a continuity equation with the probability current

$$J_i = - \sum_j M_{ij} \left( \partial_{\eta_j} \mathcal{H} + \frac{1}{\beta} \partial_{\eta_j} \right) \rho, \quad (31)$$

and where the matrix  $M$  reads

$$M_{ij} \equiv \beta \Gamma_i \delta_{ij} - A_{ij}. \quad (32)$$

In order to calculate the nucleation rate, one must solve Eq. (30). A particular solution is obtained at equilibrium and is given by the Maxwell-Boltzmann distribution

$$\rho_{eq} = \exp(-\beta \mathcal{H} \{\eta\}) / Z_0, \quad (33)$$

which corresponds to zero current,  $J_i = 0$ . However, what is really needed is to obtain a finite probability current flowing across the saddle point  $\eta^{(s)}$ . As stated above, considering a steady-state so that the rate at which the metastable state is replenished is equal to the rate of leak across the activation-energy barrier, the problem then consists in finding this steady-state as a solution of Eq. (30) in the immediate neighborhood of the saddle point. To obtain this solution, it is more convenient to work in the frame of canonical coordinates with their origin at  $\eta^{(s)}$ , defined by

$$\xi_n = \sum_i \mathcal{D}_{ni} (\eta_i - \eta_i^{(s)}), \quad (34)$$

where the transformation matrix  $\mathcal{D}$  diagonalizes the energy Hessian, so that the energy can be rewritten near  $\{\xi\} = \{0\}$  as

$$E_s \simeq E_s^{(0)} + \frac{1}{2} \sum_{n=1}^N \lambda_n \xi_n^2. \quad (35)$$

The  $\lambda_n$ 's are the eigenvalues of the energy Hessian. By the definition of  $\eta^{(s)}$ , one of the  $\lambda$ 's, denoted in the sequel by  $\lambda_-$ , is negative; that is, the energy at the saddle point diminishes on either side of the surface  $\xi_- = 0$ . Moreover, we expect that  $m < N$  eigenvalues vanish, which corresponds to the fact that the saddle point does not possess all of the symmetries of  $\mathcal{H} \{\eta\}$ . The unbroken symmetries produce Goldstone modes<sup>3</sup> that must be eliminated from the nucleation rate as they cause the latter to diverge. Consequently, the saddle point is actually a bounded, finite-dimensional subspace of the  $\eta$ -space. The volume of this subspace will be denoted below by  $\mathcal{V}$ . For the single-spin problem, this is just the space spanned by rotations around the angle  $\varphi$ , while  $\cos \theta^{(s)} = -h$ , and its volume is given by  $\mathcal{V}_s = 2\pi \sin \theta^{(s)} = 2\pi \sqrt{1 - h^2}$ .

Next, one diagonalizes the transition matrix that results from the dynamical equation (28) linearized at the saddle point, that is one has to solve the eigenvalue problem:

$$\lambda_n \sum_m \tilde{M}_{nm} U_m = \kappa U_n, \quad (36)$$

---

<sup>3</sup> A spontaneous breaking of a continuous symmetry entails the existence of a massless mode, that is a zero-energy fluctuation, called the Goldstone mode: This is the well-known Goldstone theorem [50].

where the prime on the summation indicates that we omit all  $n$ 's for which  $\lambda_n = 0$ , and

$$\tilde{M}_{nm} \equiv \sum_{i,j} \mathcal{D}_{ni} (-A_{ij}) \mathcal{D}_{mj} = -\tilde{M}_{nm}. \quad (37)$$

As was argued by Langer [49], one, and only one, of the eigenvalues  $\kappa$  must be negative. Indeed, if the saddle point is to describe the nucleating fluctuation, there must be exactly one direction of motion away from the saddle point  $\{\xi\} = \{0\}$  in which the solution

$$\langle \xi_m \rangle = X_n e^{-\kappa t}, \quad (38)$$

of the equation of motion of the  $\xi_n$  modes

$$\frac{d \langle \xi_n \rangle}{dt} = - \sum_m \tilde{M}_{nm} \lambda_m \langle \xi_m \rangle, \quad (39)$$

is unstable.

Finally,  $Z_0$  in Eq. (33) is a normalization factor defined by the condition that the equilibrium probability density (33) is normalized at the metastable state, i.e.,

$$\frac{1}{Z_0} \int_{\eta^{(m)}} \mathcal{D}\eta \exp(-\beta \mathcal{H}^{(m)}\{\eta\}) = 1,$$

which leads to

$$Z_0 \simeq e^{-\beta E_m^{(0)}} \prod_{l=1}^4 \left( \frac{2\pi}{\beta \lambda_l^{(m)}} \right)^{1/2}, \quad (40)$$

where  $\lambda_l^m$  are the eigenvalues of the energy Hessian at the metastable state and  $E_m^{(0)}$  its energy.

Taking all this into consideration, Langer has given a formula for the switching rate  $\Gamma$  out of the metastable state which reads,

$$\Gamma = \frac{\mathcal{V}}{2\pi} \sqrt{\frac{\beta}{2\pi}} \frac{|\kappa|}{\sqrt{|\lambda_-|}} \left( \prod_l \sqrt{\lambda_l^m} \right) \left( \prod_n'' \frac{1}{\sqrt{\lambda_n}} \right) \times e^{-\beta \Delta E_0}, \quad (41)$$

where  $\Delta E_0 \equiv E_0^{(s)} - E_0^{(m)}$  is the barrier energy between the saddle point and the metastable state, and the double prime on the product symbol indicates that we omit the negative eigenvalue  $\lambda_-$  and all  $n$  for which  $\lambda_n = 0$ .

The whole procedure can be summarized as follows: From a static study of the energy, one identifies the metastable states and saddle points. Then at a given saddle point one expands the energy to second order, calculates the Hessian and its eigenvalues. The vanishing eigenvalues corresponding to the Goldstone modes, associated with the unbroken symmetries at the saddle point, are eliminated from the final expression of the relaxation rate. The volume  $\mathcal{V}$  of the saddle-point subspace is also calculated. Then, one solves the eigenvalue problem (36) and obtains the negative eigenvalue  $\kappa$ . Finally, one calculates the eigenvalues  $\lambda_l^m$  of the Hessian of energy expanded at the metastable state.

A quite similar approach has been used by D.A. Garanin [53] to calculate the thermo-activation rate of charged particles in a magnetic field. Here, the Fokker-Planck equation is written in terms of the 6 variables, 3 spatial coordinates and 3 momenta, and then linearized near the saddle point. The problem then amounts to computing the flux and normalization in the wells rendering a compact expression for the rate in terms of the frequencies in the wells and at the saddle point.

### 3.2 Relaxation rate for the two-spin problem within Langer's approach

We consider a system of two (classical) exchange-coupled spins with the Hamiltonian

$$\mathcal{H} = -\frac{j}{2}\vec{s}_1 \cdot \vec{s}_2 - \frac{1}{2} \left[ (\vec{s}_1 \cdot \vec{e}_1)^2 + (\vec{s}_2 \cdot \vec{e}_2)^2 \right] - \vec{h} \cdot (\vec{s}_1 + \vec{s}_2),$$

$$j \equiv J/K, h \equiv H/2K \quad (42)$$

where  $J > 0$  is the exchange coupling,  $K > 0$  the anisotropy constant,  $H$  the applied magnetic field, and  $h$  the reduced field, i.e.,  $0 \leq h < 1$ .  $\vec{e}_i$  are uniaxial anisotropy unit vectors. We use the dimensionless units, i.e.,  $[\mathcal{H}] = 2K$  for energy and  $[t] = 1/(2\gamma K)$  for time. Here we restrict ourselves to the case  $\vec{h} \parallel \vec{e}_i, i = 1, 2$ , with the same anisotropy constant. Owing to the symmetry of this system with respect to rotations around the easy axis, the number of variables reduces to three,  $\theta_1, \theta_2, \varphi \equiv \varphi_1 - \varphi_2$ .

Now we apply Langer's approach to the energy (42) and study the relaxation rate as a function of the exchange coupling  $j$ . We first analyze the energyscape in Fig. 5. The absolute minimum of the energy (42) corresponds to the ferromagnetic ordering of the two spins along the easy axis,

$$(0, 0, \varphi); \quad e_{ss}^{(0)} = -\frac{j}{2} - 2h - 1, \quad (43)$$

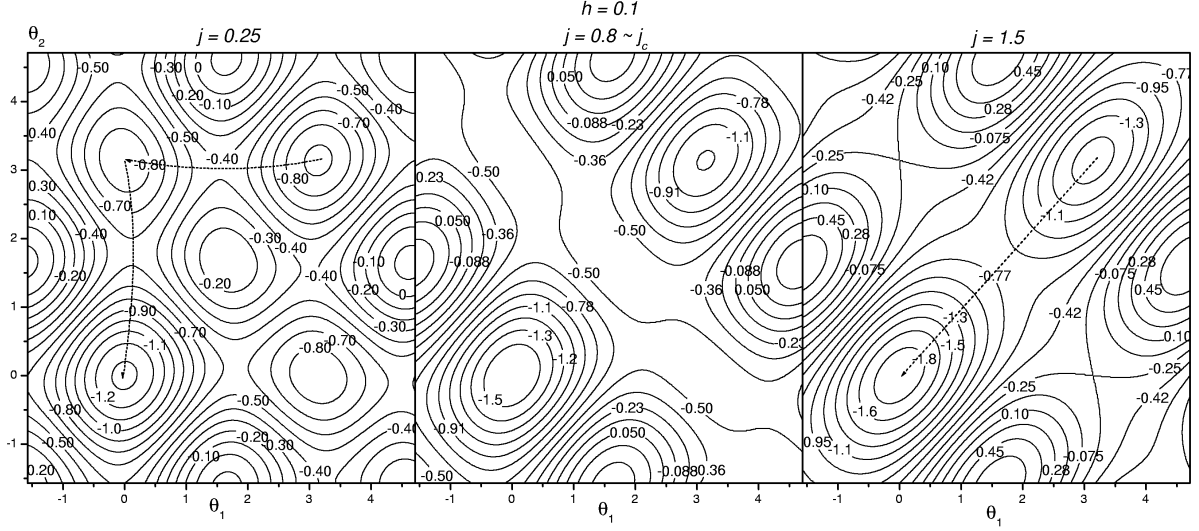


Fig. 5. Energyscape from Eq. (42) ( $\varphi = 0$ ) for  $j = 0.25, 0.8, 1.5$  and  $h = 0.1$ . The arrows indicate the switching paths.

where henceforth  $e^{(0)}$  denotes the energy of the state. One metastable state corresponds to a ferromagnetic ordering opposite to the field

$$(\pi, \pi; \varphi); \quad e_{m_1}^{(0)} = -\frac{j}{2} + 2h - 1. \quad (44)$$

There is also the metastable state of anti-ferromagnetic ordering,

$$(0, \pi; \varphi) \text{ or } (\pi, 0; \varphi); \quad e_{m_2}^{(0)} = \frac{j}{2} - 1. \quad (45)$$

As to saddle points, we find that their number and loci crucially depend on the exchange coupling constant  $j$ . More precisely, for  $j > j_c \equiv 1 - h^2$ , there is a single saddle point given by

$$(\cos \theta_1 = \cos \theta_2 = -h; \varphi); \quad e_s^{(0)} = -\frac{j}{2} + h^2, \quad (46)$$

whereas for  $j < j_c$  there are two saddle points given by

$$\cos \theta_{1,2}^\varepsilon = \frac{1}{2} \left( -h - a^\varepsilon \pm \sqrt{\Delta^\varepsilon} \right) \equiv X_\pm^\varepsilon; \quad \varphi, \quad (47)$$

where  $\varepsilon = \pm$  and



$$a^\varepsilon = \varepsilon \sqrt{1-j} \quad b^\varepsilon = \varepsilon \sqrt{1 + \frac{(j/2)^2}{1-j}}$$

$$\Delta^\varepsilon = (h + a^\varepsilon)^2 + 2j - 4b^\varepsilon h,$$

with energy,

$$e_\varepsilon^{(0)} = -\frac{j}{2} \sqrt{(1 + b^\varepsilon h - \frac{j}{2})^2 - (a^\varepsilon + h)^2} - \frac{j}{2} (1 + b^\varepsilon h - \frac{j}{2})$$

$$+ \frac{1}{2} (h^2 - (a^\varepsilon)^2 + 2b^\varepsilon h). \quad (48)$$

At  $j = j_c$  the saddle point (47) with  $\varepsilon = +$  merges with the saddle point (46), while that with  $\varepsilon = -$  merges with the metastable state (45), see Fig. 5 central panel.

Starting with both spins aligned in the metastable state (44) with  $\theta_{1,2} = \pi$ , if  $j < j_c$  one of the two spins crosses the saddle point (47) ( $\varepsilon = +$ ) into the state (45) by reversing its direction. Then the second spin follows through the second saddle point (47) ( $\varepsilon = -$ ), of lower energy due to the exchange coupling (see Fig. 6), ending up in the stable state (43). In Fig. 5 (left) the path is indicated by a pair of curved arrows. There are actually two such paths corresponding to the two-fold symmetry of the problem owing to the full identity of the two spins. Note that when the first spin starts to switch and arrives at  $\theta_1 \sim \pi/2$ , the second spin has  $\theta_2 \lesssim \pi$  (hence the curved arrows in Fig. 5), which suggests that in the switching process of the first spin, the position of the second spin undergoes some fluctuations creating a small transverse field, and when  $\theta_1 = 0$  the second spin goes back to the position  $\theta_2 = \pi$  before it proceeds to switch in turn. The successive switching of the two spins through the corresponding saddle points is a sequential two-step process<sup>4</sup>, so the relaxation rates for  $j < j_c$  add up inverse-wise. In the case  $j > j_c$  the two spins cross the unique saddle point (46) to go from the metastable state (44) into the stable one (43) in a single step, see Fig. 5 (right) where the path is indicated by a single straight arrow. There is the symmetry  $\pm\theta^{(s)}$ , which leads to a factor of 2 in the relaxation rate. Therefore, if we denote by  $\Gamma_{j \leq j_c}^+$ ,  $\Gamma_{j \leq j_c}^-$ , and  $\Gamma_{j \geq j_c}$  the respective relaxation rates, the relaxation rate of the two-spin system can then be written as

$$\Gamma = \begin{cases} 2\Gamma_{j \leq j_c}^+ \Gamma_{j \leq j_c}^- / (\Gamma_{j \leq j_c}^+ + \Gamma_{j \leq j_c}^-), & \text{if } j \leq j_c \\ 2\Gamma_{j \geq j_c}, & \text{if } j \geq j_c. \end{cases} \quad (49)$$

<sup>4</sup> Similarly, it was found in Ref. [48] that the reversal of the two dipoles considered is a two-stage process with an intermediary metastable antiparallel state.

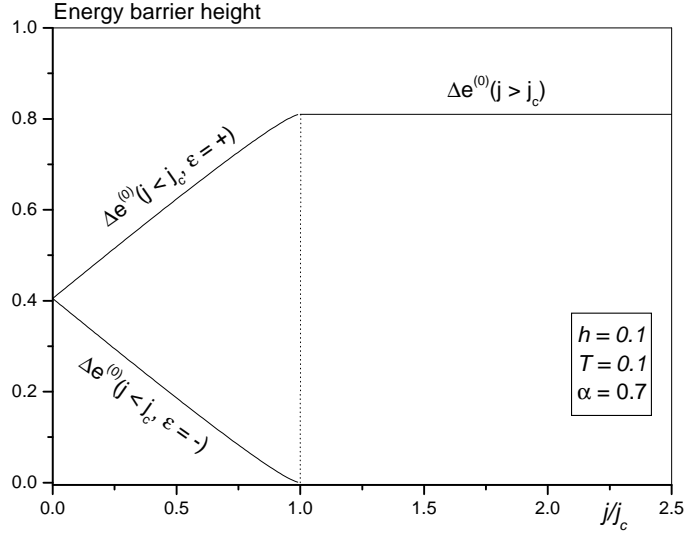


Fig. 6. Energy barrier as a function of  $j$ .

In Langer's approach the  $\Gamma$ 's in Eq. (49) are obtained from the steady-state Fokker-Planck equation (SSFPE) linearized around each saddle point, using the fluctuating variables  $\eta_i = (t_i, p_i)$  where  $t_i \equiv \theta_i - \theta_i^s$ ,  $p_i \equiv \varphi_i - \varphi_i^s$ ,  $i = 1, 2$ , or more adequately the "canonical" variables  $\psi_n = (\xi_{\pm}, \zeta_{\pm})$  with  $\xi_{\pm} = (t_1 \pm t_2)/\sqrt{2}$ ,  $\zeta_{\pm} = (p_1 \pm p_2)/\sqrt{2}$ , in which the energy Hessian is diagonal.

The deterministic dynamic of the system is governed by the Landau-Lifshitz equations, which upon linearization near the saddle point, read

$$\begin{cases} \partial_t t_i = -\partial_{p_i} \mathcal{H}_2 - \alpha \partial_{t_i} \mathcal{H}_2 \\ \partial_t p_i = -\alpha \partial_{p_i} \mathcal{H}_2 + \partial_{t_i} \mathcal{H}_2, \quad i = 1, 2 \end{cases} \quad (50)$$

where  $\mathcal{H}_2$  is the quadratic approximation of the energy (42) near the saddle point and  $\alpha$  is the damping parameter. In matrix form Eqs. (50) become

$$\partial_t \eta_i = \sum_j M_{ij} \partial_{\eta_j} \mathcal{H}_2, \quad (51)$$

where  $M$  is the dynamic matrix containing the precessional and dissipative parts. Rather than investigating the stochastic trajectories  $\eta_i(t)$  that arise by adding a noise term in Eq. (51), Langer concentrates on the distribution function  $\rho(\{\eta\}, t)$  as the probability that the system is found in the configuration  $\{\eta\}$  at time  $t$ . The time evolution of  $\rho$  is governed by the Fokker-Planck equation (30), where now the current  $J_i$  is given by Eq. (31) with the Hamiltonian  $\mathcal{H}$  replaced by its quadratic approximation  $\mathcal{H}_2$ .

Instead of solving the time-dependent equation (30), Langer solves the SSFPE  $\partial_t \rho = 0$  near the saddle point. The steady-state is realized by imposing the boundary conditions:  $\rho \simeq \rho_{eq}$  near the metastable state and  $\rho \simeq 0$  beyond the saddle point. Then, the problem of calculating the escape rate boils down to the calculation of the total current by integrating the probability current (31) over a surface through the saddle point. After performing all these steps, Langer arrives at his famous expression (41) for the relaxation rate which is valid in the IHD limit. The general calculations can be found in greater details in [49], or applied to magnetic particles in [51], see also the review article [52].

However, since the escape rate is simply given by the ratio of the total current through the saddle point to the number of particles in the metastable state, it turns out that Langer's result for the escape rate can be retrieved by only computing the energy-Hessian eigenvalues near the saddle points and metastable states, from which one then infers the partition function  $\tilde{Z}_s$  of the system restricted to the region around the saddle point where the energy-Hessian negative eigenvalue is (formally)<sup>5</sup> taken with absolute value, and the partition function  $Z_m$  of the region around the metastable state. When computing these partition functions, one has to identify and take care of the Goldstone modes associated with the unbroken global symmetries of the different states. Finally, one computes the unique negative eigenvalue  $\kappa$  of the SSFPE corresponding to the unstable mode at the saddle point. More precisely,  $\kappa$  is given by the negative eigenvalue of the dynamic matrix  $\tilde{M}_{mn} = -\lambda_n (\mathcal{D} M \mathcal{D}^T)_{mn}$ , where the  $\lambda_n$ 's are the eigenvalues of the Hessian at the saddle point and  $\mathcal{D}$  is the transformation matrix from  $\eta_i$  to  $\psi_n$  [see Eq. (34)].

Consequently, Langer's final expression for the escape rate is rewritten in the following somewhat more practical form

$$\Gamma = \frac{|\kappa|}{2\pi} \frac{\tilde{Z}_s}{Z_m}, \quad (52)$$

where  $|\kappa|$  is the attempt frequency which contains the damping parameter  $\alpha$ .

### 3.3 Relaxation rate of the two-spin system

Now, we give the different relaxation rates for  $j > j_c$ ,  $j < j_c$ , and  $j \simeq j_c$ .

---

<sup>5</sup> See Ref. [49] for a rigorous derivation

### 3.3.1 Relaxation rate for $j > j_c$

The quadratic expansion of the energy (42) at the saddle point (46) reads,

$$H_s^{(2)} = e_s^{(0)} - \frac{j_c}{2}\xi_+^2 + \frac{j-j_c}{2}\xi_-^2 + \frac{jj_c}{2}\zeta_-^2, \quad (53)$$

with zero eigenvalue for the  $\zeta_+$  mode, that is the Goldstone mode associated with the rotation around the easy axis.  $e_s^{(0)}$  is given in Eq. (46). The negative eigenvalue of the SSFPE, corresponding to the unstable mode, is  $\kappa = -\alpha j_c$ .

The partition function around the saddle point  $Z_s = \int d\Omega_1 d\Omega_2 e^{-\beta H_s^{(2)}}$ , where  $d\Omega_i = \sin\theta_i d\theta_i d\varphi_i$ ,  $i = 1, 2$  is calculated by changing to the variables  $\xi_{\pm}, \zeta_{\pm}$ , setting  $\sin\theta_i \simeq \sqrt{j_c}$  (see Eq. (46)) in the integration measure, and substituting  $2\pi$  for the integral over  $\zeta_+$ , and finally computing the Gaussian integrals. Hence,

$$\tilde{Z}_s = 2\pi \left(\frac{2\pi}{\beta}\right)^{3/2} \frac{1}{j\sqrt{1-j_c/j}} e^{-\beta e_s^{(0)}}, \quad (54)$$

where we have formally replaced the negative eigenvalue  $(-j_c)$  by its absolute value. Next, the partition function  $Z_m$  at the (well defined) metastable state (44) is computed by expanding the energy up to  $2^{nd}$  order, leading to

$$Z_m = e^{-\beta e_{m1}^{(0)}} \left(\frac{2\pi}{\beta}\right)^2 \frac{1}{(1-h)(j+1-h)}. \quad (55)$$

Finally, using Eq. (52), the relaxation rate for  $j > j_c$  reads, upon inserting the symmetry factor of 2,

$$\begin{aligned} \Gamma_{j>j_c} &= 2\alpha \sqrt{\frac{\beta}{2\pi}} (1-h^2)(1-h) \frac{1+(1-h)/j}{\sqrt{1-j_c/j}} \times e^{-\beta \Delta e^{(0)}}, \\ \Delta e^{(0)} &= (1-h)^2. \end{aligned} \quad (56)$$

It is readily seen that for  $j \rightarrow \infty$  (56) tends to the Néel-Brown result,

$$\Gamma_{j>j_c} \rightarrow 2\alpha \sqrt{\frac{\beta}{2\pi}} (1-h^2)(1-h) e^{-\beta(1-h)^2}, \quad (57)$$

for the relaxation rate of one rigid pair of spins with a barrier height twice that of one spin. In fact, the result (57) coincides with the Néel-Brown result

in Eq. (23) upon reinstating the energy and time units and remembering that the result (57) is for the one-way barrier crossing. Note that the convergence of (56) to (57) is so slow that  $\Gamma_{j>j_c}$  remains above the Néel-Brown result and only merges with it for  $j \gtrsim 10$ . This confirms the fact that the one-spin approximation is only valid for extremely large exchange interaction.

### 3.3.2 Relaxation rate for $j < j_c$

Here the attempt frequencies  $|\kappa^\varepsilon|$  (for  $\varepsilon = \pm$ ) cannot be obtained in a closed form and are thus computed numerically, this means that the present case can only be dealt with semi-analytically. On the other hand, following the same procedure as for  $j > j_c$  we obtain the relaxation rate for  $\varepsilon = \pm$ ,

$$\Gamma_{j<j_c}^\varepsilon = \sqrt{\frac{\beta}{\pi}} |\kappa^\varepsilon| \sqrt{\frac{P^\varepsilon}{j}} \frac{N^\varepsilon}{\sqrt{R_+^\varepsilon R_-^\varepsilon + jQ^\varepsilon(R_+^\varepsilon + R_-^\varepsilon)}} e^{-\beta\Delta e_\varepsilon^{(0)}}, \quad (58)$$

where  $\Delta e_\varepsilon^{(0)}$  is the barrier height given by the energy (48) measured with respect to (44) or (45) for  $\varepsilon = +, -$  respectively, and (see Eq. (47) et seq. for notation)

$$\begin{aligned} P^\varepsilon &= \sqrt{(1 + b^\varepsilon h - j/2)^2 - (a^\varepsilon + h)^2}, \\ Q^\varepsilon &= b^\varepsilon h - j/2 + P^\varepsilon, \quad R_\pm^\varepsilon = -1 + X_\pm^\varepsilon(2X_\pm^\varepsilon + h), \\ N^+ &= (1 - h)(j + 1 - h), \quad N^- = j_c - j. \end{aligned}$$

The limit of the relaxation rate (58) when  $j \rightarrow 0$  is just the Néel-Brown result for one spin. Indeed, the product of the last two factors in the prefactor tend to  $(1 - h)/\sqrt{2}$ , the attempt frequencies tend to  $\alpha j_c = \alpha(1 - h^2)$ , and the energy barriers  $\Delta e_\varepsilon^{(0)} \rightarrow (1 - h)^2/2$ .

Note that in the present regime of  $j < j_c$  the large value of anisotropy has not changed the temperature dependence of the individual relaxation rates, i.e.,  $\Gamma_{j<j_c}^\varepsilon$ , with  $\varepsilon = \pm$ . This is due to the fact that  $1/\sqrt{T}$  appears in the prefactor each time there is a continuously degenerate class of saddle points [51], which is indeed the case for  $j > j_c$  and  $j < j_c$  with  $\varepsilon = +$  and  $\varepsilon = -$ . However, anisotropy do affect the temperature dependence of the relaxation rate of the two-spin system, since for  $j < j_c$  there are two saddle points bringing each a factor  $1/\sqrt{T}$ , see the first line in Eq. (49).

### 3.3.3 The case of $j \simeq j_c$

When  $j$  approaches  $j_c$  either from above or from below, more Hessian eigenvalues (in addition to  $\lambda_{\zeta^+}$ ) vanish, rendering the saddle point rather flat and

thus leading to a divergent relaxation rate. Indeed, for  $j \simeq j_c$  the relaxation rate (56) diverges, which clearly shows that Langer's approach making use of a quadratic approximation for the energy at the saddle point, e.g., Eq. (53), fails in this case. The remedy is to push the energy expansion to the 6<sup>th</sup>-order in the variable  $\xi_-$  (since  $\lambda_{\xi_-} = j - j_c \rightarrow 0$  as  $j \rightarrow j_c$ ), i.e.,

$$\delta e_s = e_s - e_s^{(0)} \simeq \frac{\lambda_{\xi_-}}{2} \xi_-^2 + \frac{c}{4} \xi_-^4 + \frac{d}{6} \xi_-^6, \quad (59)$$

where

$$c = \frac{1 - j - 7h^2/4}{3} < 0, \quad d = \frac{j - 1 + 31h^2/16}{30} > 0.$$

Then, the contribution  $\sqrt{2\pi/\beta\lambda_{\xi_-}}$  of the mode  $\xi_-$  to the relaxation rate (56) must be replaced by  $\int_{-\infty}^{\infty} d\xi_- e^{-\beta\delta e}$ , upon which the divergence of  $\Gamma_{j>j_c}$  is cut out (see Fig. 7).

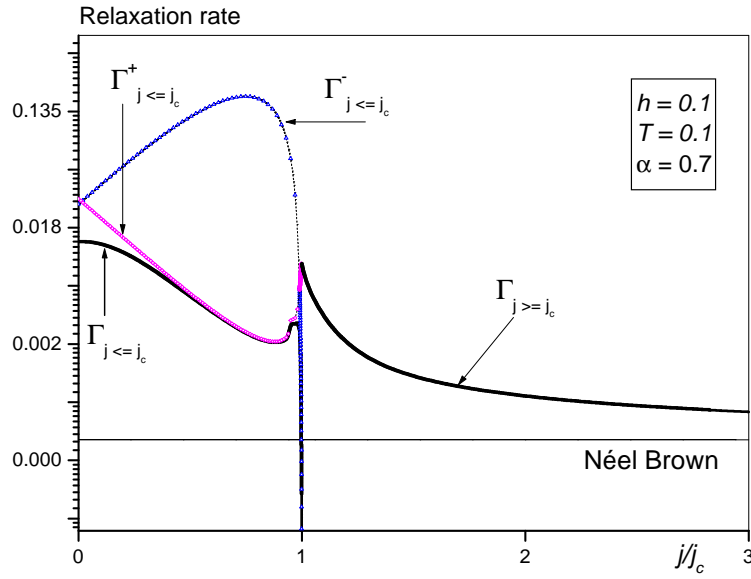


Fig. 7. Relaxation rate (in logarithmic scale) of the two-spin system in the case of intermediate-to-high damping. The horizontal line is the Néel-Brown result with the barrier height taken twice that of a single spin.

Similarly, when  $j$  approaches  $j_c$  from below, for  $\varepsilon = -$  the eigenvalue  $\lambda_{\xi_-}$  vanishes at  $j = j_c$ , upon which the saddle point (47) ( $\varepsilon = -$ ) merges with the state (45) and thereby the partition functions  $\tilde{Z}_s$  and  $Z_m$  tend to infinity. However, as  $Z_m \propto 1/(j_c - j)$  increases much faster than  $\tilde{Z}_s$ , and  $|\kappa^-| \rightarrow 0$ ,  $\Gamma_{j<j_c}^-$  tends to zero as  $j \rightarrow j_c$ . On the other hand, for  $\varepsilon = +$ , both  $\lambda_{\xi_-}$  and  $\lambda_{\xi_+}$  vanish leading to a divergent relaxation rate, since now  $\tilde{Z}_s$  diverges but  $Z_m$  in

Eq. (55) remains finite for the metastable state (44) is well defined. Indeed, as  $j \rightarrow j_c$ , the relaxation rate  $\Gamma_{j < j_c}^+$  goes over to the result in Eq. (56) upon making the change  $j \leftrightarrow j_c$ , and taking account of the symmetry factor. In this case, the divergence at the point  $j = j_c$  cannot be cut off by expanding the energy beyond the 2<sup>nd</sup> order and  $\Gamma_{j < j_c}^+$  is simply cut off at the point where it joins  $\Gamma_{j > j_c}$  taking account of Eq. (59).

In Fig. 7 we plot ( $\ln$  of) the relaxation rate of the two-spin system as defined in Eq. (49), under the condition of IHD, in which Langer's approach is valid, that the reduced barrier height  $\beta\Delta e^{(0)} \gg 1$  and  $\alpha\beta\Delta e^{(0)} > 1$  [52]. We also plot separately both relaxation rates for  $j \leq j_c$ . We see that the relaxation rate of the two-spin system contains two unconnected branches corresponding to the two regimes,  $j < j_c$  and  $j > j_c$ , the bridging of which would require a more sophisticated approach. Fig. 7 also shows that as  $j$  increases, but  $j \ll j_c$ , the relaxation rate  $\Gamma_{j \leq j_c}^+$  decreases because the switching of the first spin is hindered by the (ferromagnetic) exchange coupling. While  $\Gamma_{j \leq j_c}^+$  is an increasing function of  $j$  with a faster rate, since now the exchange coupling works in favor of the switching of the second spin. This is also illustrated by the evolution of the energy barrier height in Fig. 6. As  $j$  approaches  $j_c$  from below, the relaxation rate  $\Gamma_{j \leq j_c}^+$  tends to  $\Gamma_{j \geq j_c}$  because the respective saddle points merge at  $j = j_c$ . Whereas  $\Gamma_{j \leq j_c}^-$  goes to zero since the corresponding saddle point merges with the antiferromagnetic state that is no longer accessible to the system. For  $j \geq j_c$ , as  $j$  increases the minimum (43), the metastable state (44) and the saddle point (46) merge together, which means that the system is found in an "energy groove" along the direction  $\theta_1 = \theta_2$  because the eigenvalue  $\lambda_{\xi_-}$  corresponding to the mode  $\theta_1 - \theta_2$  becomes very large, and thus the escape rate decreases and eventually reaches the Néel-Brown value at large  $j$ .

#### 4 Discussion: What is wrong with the one-spin approximation ?

We have seen that the magnetization of a nanoparticle can overcome the energy barrier and thus reverse its direction, at least in two ways: either under applied magnetic field which suppresses the barrier, or through thermally activated statistical fluctuations. Within the framework of the one-spin approximation, the magnetization switching under applied field, at zero temperature, is well described by the Stoner-Wohlfarth model. At finite temperature and short-time scales, crossing of the energy barrier activated by thermal fluctuations is described by the Néel-Brown model and its extensions reviewed above. Both of these models have been confirmed by experiments on individual cobalt particles [6]. At finite temperature, but at quasi-equilibrium, the magnetization switching occurs according to two distinct regimes. At very low temperature, this is due to the coherent rotation of all spins, as in the Stoner-Wohlfarth model, whereas at higher temperature, the magnetization switches

by changing its magnitude. This results in a shrinking of the Stoner-Wohlfarth astroid as described by the modified Landau theory [7], and confirmed by experiments [6]. However, it is clear that the change of magnetization magnitude cannot be explained in the framework of the one-spin approximation. Indeed, it can only be understood as the result of a successive switching of individual (or clusters of) spins inside the particle, which is necessarily a multi-spin system. Indeed, deviations from the single-spin approximation, and thereby from both the Stoner-Wohlfarth and Néel-Brown models, have been observed in metallic particles [54], [55], and ferrite particles [56], [57]. These deviations have materialized in terms of the absence of magnetization saturation at high fields, shifted hysteresis loops after cooling in field, and enhancement at low temperature of the magnetization as a function of applied field. The latter effect has been clearly identified in dilute assemblies of maghemite particles [58] of 4 nm in diameter. In addition, aging effects have been observed in cobalt single particles and have been attributed to the oxidation of the sample surface into antiferromagnetic CoO or NiO [see Ref. [6] and references therein for a discussion of this issue]. It was argued that the magnetization reversal of a ferromagnetic particle with antiferromagnetic shell is governed by two mechanisms that are supposed to be due to the spin frustration at the core-shell interface of the particle. On the other hand, according to Mössbauer spectroscopy some of the above-mentioned novel features are most likely due to magnetic disorder at the surface which induces a canting of spins, or in other words, an inhomogeneous magnetic state inside the particle.

As argued earlier, understanding these effects requires the development of microscopic theories capable of distinguishing and accounting for the various crystallographic local environments that develop inside a nanoparticle and on its surface. Elaboration of such theories is faced with tough non-linear  $N$ -body problems whose study can only be, in principle, efficiently performed with the help of numerical approaches. It is however desirable, and indeed even necessary, that the numerical calculations be backed by analytical expressions, in some limiting cases at least.

Accordingly, the study of section 3 has helped us understand the effect of exchange coupling on the relaxation rate of the two-spin system. The corresponding analytical results will be very helpful in a generalization to multi-spin small particles at least for small values of surface anisotropy and thereby small deviations from collinearity, where it has been shown [59] that the surface contribution to the macroscopic energy has a simple cubic anisotropy. However, this generalization can only be performed using numerical techniques. This is now attempted by the help of the ridge method [60] for probing the potential energy surface and locating the saddle points, and by the (Onsager-Machlup) path integrals [61] for determining the most probable paths connecting a metastable state to a more stable state.



## 5 acknowledgments

I would like to thank my colleagues W.T. Coffey, D.A. Garanin, M. Noguès, E. Tronc, and W. Wernsdorfer for fruitful collaborations.

## References

- [1] L. Néel, Ann. Geophys. 5 (1949) 99; Compt. Rend. Acad. Sci. 228 (1949) 664.
- [2] W. F. Brown, Phys. Rev. 130 (1963) 1677.
- [3] W. F. Brown, IEEE Trans. Magn. 15 (1979) 1196.
- [4] H.W. Schumacher et al., Phys. Rev. Lett. 90 (2003) 17201; 17204.
- [5] E. C. Stoner and E. P. Wohlfarth, Philos. Trans. R. Soc. London, Ser. A240 (1948) 599; IEEE Trans. Magn. MAG-27 (1991) 3475.
- [6] W. Wernsdorfer, Adv. Chem. Phys. 118 (2001) 99.
- [7] H. Kachkachi and D. A. Garanin, Physica A291 (2001) 485.
- [8] W.F. Brown Jr. and A.H. Morrish, Phys. Rev. 105 (1957) 1198.
- [9] H. Kachkachi and D. A. Garanin, Physica A300 (2001) 487. H. Kachkachi and M. Dimian, Phys. Rev. B66 (2002) 174419.
- [10] A. Thiaville, J. Magn. Magn. Mater. 182 (1998) 5; Phys. Rev. B61 (2000) 12221.
- [11] L.N Bulaevskii and V.L. Ginzburg, Zh. Eksp. Teor. Fiz. 45 (1963) 772; JETP 18 (1964) 530.
- [12] J. Kötzler, D. A. Garanin, M. Hartl, and L. Jahn, Phys. Rev. Lett. 71 (1993) 177.
- [13] M. Jamet, W. Wernsdorfer, C. Thirion, D. Mailly, V. Dupuis, P. Mélinon, and A. Pérez, Phys. Rev. Lett. 86 (2001) 4676.
- [14] J. H. Van't Hoff, in *Etudes de Dynamiques Chimiques*, edited by F. Muller and Co., Amsterdam, 1884.
- [15] S. Arrhenius, Z. Phys. Chem. 4 (1889) 226.
- [16] A. Aharoni, *Introduction to the theory of ferromagnetism*, Oxford Science Pubs., 1996.
- [17] J.L. Garcia-Palacios, Adv. Chem. Phys. 112 (2000) 1.
- [18] H. A. Kramers, Physica, 7 (1940) 284.

- [19] V.I. Mel'nikov and S.V. Meshkov, J. Chem. Phys. 85 (1986) 1018.
- [20] M. Büttiker, E.P. Harris, and R. Landauer, Phys. Rev. B28 (1983) 1268.
- [21] P. Hänggi, P. Talkner, and M. Borkovec, Rev. Mod. Phys. 62 (1990) 251.
- [22] I. Klik and L. Gunther, J. Appl. Phys. 67 (1990) 4505.
- [23] L.J. Geoghegan, W.T. Coffey, and B. Mulligan, Adv. Chem. Phys. 100 (1997) 475.
- [24] W.T. Coffey, D.S.F. Crothers, J.L. Dormann, L.J. Geoghegan, Yu.P. Kalmykov, J.T. Waldron, and A.W. Wickstead, Phys. Rev. B52 (1995) 15951.
- [25] W.T. Coffey, D.S.F. Crothers, J.L. Dormann, L.J. Geoghegan, and E.C. Kennedy, Phys. Rev. B58 (1998) 3249.
- [26] W.T. Coffey, D.S.F. Crothers, J.L. Dormann, Yu.P. Kalmykov, E.C. Kennedy, and W. Wernsdorfer, Phys. Rev. Lett. 80 (1998) 5655.
- [27] W.T. Coffey Adv. Chem. Phys. 103 (1998) 259.
- [28] W.T. Coffey, D.S.F. Crothers, J.L. Dormann, L.J. Geoghegan, E.C. Kennedy, and W. Wernsdorfer, J. Phys. C 10 (1998) 9093.
- [29] A. Aharoni Phys. Rev. 135A (1964) 447.
- [30] A. Aharoni, Phys. Rev. 177 (1969) 793.
- [31] W.F. Brown Jr., Physica B86-88 (1977) 1423.
- [32] C.N. Scully, P.J. Cregg, and D.S.F. Crothers, Phys. Rev. B45 (1992) 474.
- [33] L. Bessais, L. Ben Jaffel, and J.L. Dormann, Phys. Rev. B45 (1992) 7805.
- [34] A. Aharoni, Phys. Rev. B46 (1992) 5434.
- [35] P.J. Cregg, D.S.F. Crothers, and A.W. Wickstead, J. Appl. Phys. 76 (1994) 4900.
- [36] D.A. Garanin, V.V. Ishchenko, and L.V. Panina, Theor. Math. Phys. 82 (1990) 169.
- [37] D.A. Garanin, Phys. Rev. B54 (1996) 3250.
- [38] D.A. Garanin, Europhys. Lett. 48 (1999) 486.
- [39] E. Kennedy, Ph.D. thesis, The Queen's University of Belfast, 1997.
- [40] H. Kachkachi, W.T. Coffey, D.S.F. Crothers, A. Ezzir, E.C. Kennedy, M. Noguès, and E. Tronc, J. Phys.: Condensed Matter 12 (2000) 3077.
- [41] D.A. Garanin, E.C. Kennedy, D.S.F. Crothers, and W.T. Coffey, Phys. Rev. E60 (1999) 6499.
- [42] W.T. Coffey, H. Kachkachi, D.A. Garanin, D.J. McCarthy, J. Magn. Magn. Mater. 221 (2000) 110.

- [43] E. Fermi, Notes on quantum mechanics, University of Chicago Press, 1965.
- [44] H. Kachkachi, Eur. Phys. Lett. 62 (2003) 650.
- [45] J.L. Dormann, L. Bessais, and D. Fiorani, J. Phys. C 21 (1988) 2015.
- [46] S. Morup and E. Tronc, Phys. Rev. Lett. 72 (1994) 3278.
- [47] P.E. Jonsson and J.L. Garcia-Palacios, Europhys. Lett. 55 (2001) 418.
- [48] A. Lyberatos and R.W. Chantrell, J. Appl. Phys. 73 (1993) 6501.
- [49] J.S. Langer, Phys. Rev. Lett. 21 (1968) 973; Ann. Phys. 54 (1969) 258.
- [50] J. Goldstone, Nuovo Cimento 19 (1961) 154; J. Goldstone, A. Salam, and S. Weinberg, Phys. Rev. 127 (1962) 965; R.V. Lange, Phys. Rev. 146 (1966) 301.
- [51] H.B. Braun, J. Appl. Phys. 76 (1994) 6310; Phys. Rev. B50 (1994) 16501.
- [52] W.T. Coffey, D.A. Garanin, D.J. McCarthy, Adv. Chem. Phys. 117 (2001) 483.
- [53] D. A. Garanin, J. Phys. I 1 (1991) 1019.
- [54] J.P. Chen, C.M. Sorensen, K.J. Klabunde, and G.C. Hadjipanayis, Phys. Rev. B51 (1995) 11527.
- [55] M. Respaud et al., Phys. Rev. B57 (1998) 2925.
- [56] R.H. Kodama and A.E. Berkovitz, Phys. Rev. B59 (1999) 6321.
- [57] J.T. Richardson, D.I. Yiagas, B. Turk, J. Forster, J. Appl. Phys. 70 (1991) 6977.
- [58] E. Tronc et al., J. Mag. Mag. Mat. 221 (2000) 63.
- [59] D.A. Garanin and H. Kachkachi, Phys. Rev. Lett. 90 (2003) 65504.
- [60] I.V. Ionova and E.A. Carter, J. Chem. Phys. 98 (1993) 6377.
- [61] D. Berkov, J. Magn. Magn. 186 (1998) 199.

